Prospects in the search for a new light Z' boson with the NA64μ experiment at the CERN SPS

H. Sieber,[1] D. Banerjee,[2] P. Crivelli,[1] E. Depero,[1] S. N. Gninenko,[3] D. V. Kirpichnikov,[3] M. M. Kirsanov,[3] V. Poliakov,[4] and L. Molina Bueno[1,5,*]

[1]*ETH Zürich, Institute for Particle Physics and Astrophysics, CH-8093 Zürich, Switzerland*
[2]*CERN, European Organization for Nuclear Research, CH-1211 Geneva, Switzerland*
[3]*Institute for Nuclear Research of the Russian Academy of Sciences, 117312 Moscow, Russia*
[4]*State Scientific Center of the Russian Federation Institute for High Energy Physics of National Research Center Kurchatov Institute (IHEP), 142281 Protvino, Russia*
[5]*CSIC—Universitat de València, Instituto de Física Corpuscular (IFIC), E-46980 Paterna, Spain*

(Received 4 November 2021; accepted 31 January 2022; published 22 March 2022)

A light Z' vector boson coupled to the second and third lepton generations through the $L_\mu - L_\tau$ current with mass below 200 MeV provides a very viable explanation in terms of new physics to the recently confirmed $(g-2)_\mu$ anomaly. This boson can be produced in the bremsstrahlung reaction $\mu N \to \mu N Z'$ after a high energy muon beam collides with a target. NA64μ is a fixed-target experiment using a 160 GeV muon beam from the CERN Super Proton Synchrotron accelerator looking for Z' production and its subsequent decays, $Z' \to$ invisible. In this paper, we present the study of the NA64μ sensitivity to search for such a boson. This includes a realistic beam simulation, a detailed description of the detectors and a discussion about the main potential background sources. A pilot run is scheduled in order to validate the simulation results. If those are confirmed, NA64μ will be able to explore all the remaining parameter space which could provide an explanation for the $g-2$ muon anomaly in the $L_\mu - L_\tau$ model.

DOI: 10.1103/PhysRevD.105.052006

I. INTRODUCTION

The recently confirmed 4.2σ deviation of the muon magnetic moment [1] with respect to its Standard Model (SM) prediction [2–22] might be an indication of physics beyond the SM:

$$\Delta a_\mu \equiv a_\mu(\text{exp}) - a_\mu(\text{th}) = (251 \pm 59) \times 10^{-11}. \quad (1)$$

Interactions between muons and new physics sectors have been suggested in many models [23–26]. In particular, models with $U(1)$ gauge extension to the SM are well motivated since they are anomaly free and provide an explanation to the $(g-2)_\mu$ anomaly through a loop contribution to the muon vertex function [27–32]. In the $L_\mu - L_\tau$ model, with SM gauge extension $SU(3)_c \otimes SU(2)_L \otimes U(1)_Y \otimes U(1)_{L_\mu - L_\tau}$ [30,33–35], the massive gauge vector boson Z' acquires its mass through symmetry breaking, $m_{Z'} \leq \mathcal{O}(1\ \text{GeV})$, and interacts to the second and third generations of leptons through

$$\mathcal{L} = g'(\bar{\mu}\gamma_\alpha\mu + \bar{\nu}_\mu\gamma_\alpha\nu_\mu - \bar{\tau}\gamma_\alpha\tau + \bar{\nu}_\tau\gamma_\alpha\nu_\tau)Z'^\alpha, \quad (2)$$

where Z'^α is the leptophilic boson field and g' is its coupling to SM leptons. Within this model, the Z' contribution to the muon vertex function, and thus the muon $(g-2)_\mu$, is calculated at one loop [36]:

$$\Delta a_\mu^{Z'} = \frac{g'^2}{4\pi^2}\int_0^1 dx \frac{x^2(1-x)}{x^2 + (1-x)m_{Z'}^2/m_\mu^2}. \quad (3)$$

The Z' vector boson decays invisibly to SM neutrinos in the case $m_{Z'} < 2m_\mu$, with decay width

$$\Gamma(Z' \to \bar{\nu}_f\nu_f) = \frac{\alpha_\mu m_{Z'}}{3}, \quad (4)$$

where $f = \mu$, τ, and $\alpha_\mu = g'^2/4\pi$. For larger Z' masses, namely $m_{Z'} \geq 2m_\mu$, the gauge boson also decays visibly to one of the charged components of the $SU(2)_L$ lepton doublets, L_μ, L_τ, with partial decay width:

*Corresponding author.
laura.molina.bueno@cern.ch

$$\Gamma(Z' \to \bar{f}f) = \frac{\alpha_\mu m_{Z'}}{3} \cdot \left(1 + \frac{2m_f^2}{m_{Z'}^2}\right) \cdot \sqrt{1 - \frac{4m_f^2}{m_{Z'}^2}}. \quad (5)$$

It is worth noting that adding to the minimal $U(1)_{L_\mu - L_\tau}$ gauge extension of the SM a dark current interaction of the type $\mathcal{L} \supset Z'^\alpha J_\alpha^{\mathrm{DM}}$ makes it possible to also probe light thermal dark matter and the dark matter (DM) relic abundance (see e.g., Ref. [37,38]).

The Z' vector boson can be produced through muon bremsstrahlung $\mu N \to \mu N Z'$ after a high energy muon beam impinges on a target. Within this context, the NA64μ experiment [37] has been designed to search for Z' production and its subsequent invisible decay using the 160 GeV M2 beam line at the CERN Super Proton Synchrotron (SPS) accelerator [39]. Detailed computations of the differential and total cross sections for this process have been recently performed in Ref. [40]. Another experiment, M^3, with a similar working principle, has been proposed at Fermilab [38]. A pilot run of the NA64μ experiment is planned in the fall of 2021 to study the feasibility of the technique. In this paper, we discuss the experiment prospects in terms of the main background sources and the expected trigger rate. We also study the projected sensitivities for future physics runs to allow to probe the region of parameter space suggested by the $(g-2)_\mu$ anomaly in the context of current and future searches.

II. THE METHOD OF SEARCH

The NA64μ experiment [37] is a complementary experiment to NA64e [41,42] aiming to look for dark sectors weakly coupled to muons. The experiment is foreseen in two phases. Its first phase physics goal is to search for invisible decays of the Z' boson, produced in the muon scattering process $\mu^- N \to \mu^- N Z'$. Additionally, similarly to the electron mode, the experiment also explores the production of dark photons, A', through the bremsstrahlung $\mu^- N \to \mu^- N A'$, allowing to enlarge the parameter space of interest towards large masses [43]. NA64μ can also probe scalar, axionlike particles (ALPs), millicharged particles [44] and could also be used to test lepton flavor violation in $\mu N \to \tau X$ conversion in flight [45]. A second phase of the experiment will be devoted to exploring these processes [37].

The experimental setup for the feasibility studies to look for a light Z' boson is sketched in Fig. 1. The experiment will use the high-energy M2 muon beam at the CERN SPS [39,46] with momentum $\simeq$160 GeV/c produced by a 450 GeV/c primary proton beam (intensity 10^{12}–10^{13} protons/spill). Within this context, muons are dumped against an active target, which is a 40 radiation lengths ($40X_0$) lead-scintillator sandwich electromagnetic calorimeter (ECAL), with a 6×5 cell matrix structure. While the scattered muon carries away a fraction $E'_\mu = fE_\mu$ of the primary muon energy E_μ, the other fraction of the energy, $(1-f)E_\mu$, is carried away by the bremsstrahlung dark boson Z' and its decay products resulting in missing energy $E_{\mathrm{miss}} = E_\mu - E'_\mu$. The subdetectors downstream of the target include, in particular, a five interaction lengths ($5\lambda_I$) copper-scintillator veto calorimeter (VHCAL) segmented with a 4×4 matrix of cells and a hole in the middle, to veto charged secondaries produced by upstream muon nuclear interactions. Then, a series of two large 120×60 cm^2 (6×3 matrix) hadronic calorimeter (HCAL) modules, with a $7.5\lambda_I$ steel-scintillator longitudinal segmentation, ensure maximal hermeticity. The experiment will use two magnet spectrometers in order to reconstruct the incoming and outgoing muon momentum. The initial muon beam momentum will be measured by the existing beam momentum stations (BMS) from the COMPASS experiment [47]. A set of micromesh gaseous structure (Micromegas or MM) tracking detectors will be located next to the stations to have a second measurement of the incoming momentum. The scattered muon momentum is reconstructed through a second MBPL magnetic spectrometer (a single dipole magnet with 1.4 T · m, MS2) with a set of six Micromegas tracking detectors.

A signal event, i.e., the production of a Z' boson, is defined as a scattered muon after the target with momentum about half of the beam nominal energy, i.e., $E'_\mu \lesssim 0.5E_0 \simeq$ 80 GeV (see Fig. 1). The muon missing momentum will be

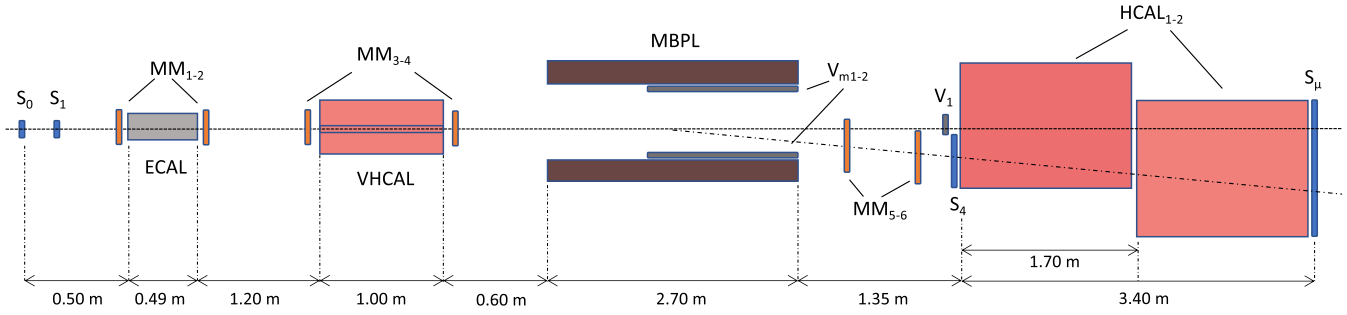

FIG. 1. Schematic top view of the 2021 muon pilot run experimental setup to search for $Z' \to$ invisible production from 160 GeV/c muon bremsstrahlung. The dash-dotted line corresponds to the path of a deflected muon after the Z' bremsstrahlung.

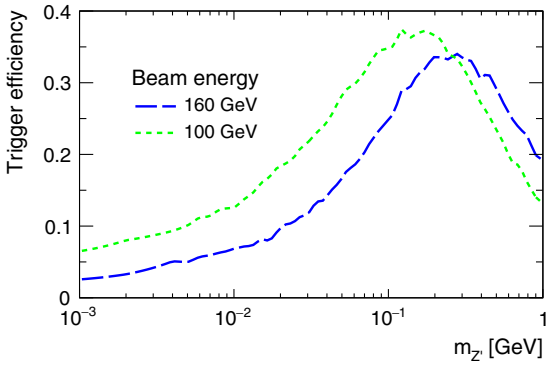

FIG. 2. Trigger efficiency as a function of the Z' vector boson mass. The beam nominal energy is both (blue) 160 GeV and (green) 100 GeV, for which the scattered muon deflection is larger.

used to keep the trigger rate at the required level. Using the deflection of the scattered muon in the transverse plane, a simplified trigger system has been considered for the initial phase to run the experiment at the low beam intensity of 10^7 μ/spill. This trigger option is based on the selection of the well-defined primary muon beam within a small beam lateral size and divergency, and momentum spread by using scintillator counters, the BMS stations and the trackers next to it. The initial muon is tagged with a set of three counters, two of them before the target (S_0 and S_1), and one ensuring the presence of the muon at the end of the setup (S_μ). An additional counter in front of the HCAL, S_4, shifted from the beam axis guarantees that only muons with enough deflection hit this counter. The signal efficiency for different Z' masses at this trigger level is illustrated in Fig. 2. A set of veto counters, before the HCAL modules (V_1), and within MS2 ($V_{m_{1,2}}$), are used to further veto undeflected beam muons and veto charged secondaries produced in upstream interactions. The trigger rate after this selection is 0.1% of the primary beam intensity.

To further suppress background coming from SM events, a set of selection criteria (cuts) is applied as follows: (i) an initial beam momentum reconstructed in the energy window [140, 180] GeV; (ii) a single track in the tracking detectors with reconstructed momentum smaller than half of the beam energy; (iii) no energy deposit in the VHCAL; and (iv) no energy deposit in the HCAL modules [i.e., compatible with the one of a minimum ionizing particle (MIP)].

III. SIMULATIONS FRAMEWORK

Detailed Monte Carlo (MC) simulations are performed using the GEANT4 toolkit [48] and the GEANT4-compatible DM package DMG4 [49] aiming at realistically reproducing the beam line, detectors and physics, as well as estimating the background and signal topology within the setup.

A. The beam profile at M2 location

Because of the importance of an accurate knowledge of the initial muon momentum and beam spatial distribution for the trigger criteria, the M2 beam line optics is fully simulated using the TRANSPORT [50], TURTLE [51] and HALO [52] software [46] and made compatible with GEANT4 through the HEPMC software [53]. This yields realistic beam profiles as shown in Fig. 3. Simulations reproduce the large contribution of low-energy halo muons around the beam spot (about 20% of the full beam intensity [37]) that are populating the low-energy tail of the beam energy distribution. Such muons can be efficiently removed using the beam-defining counters S_0 and S_1, leaving 78% of the full beam intensity, with muons energy $\geq$100 GeV, with beam spot divergency $\sigma_x \sim 0.9$ cm and $\sigma_y \sim 1.9$ cm.

B. Signal

To estimate both the signal yield and signal topology, and thus the choice of adequate selection criteria,

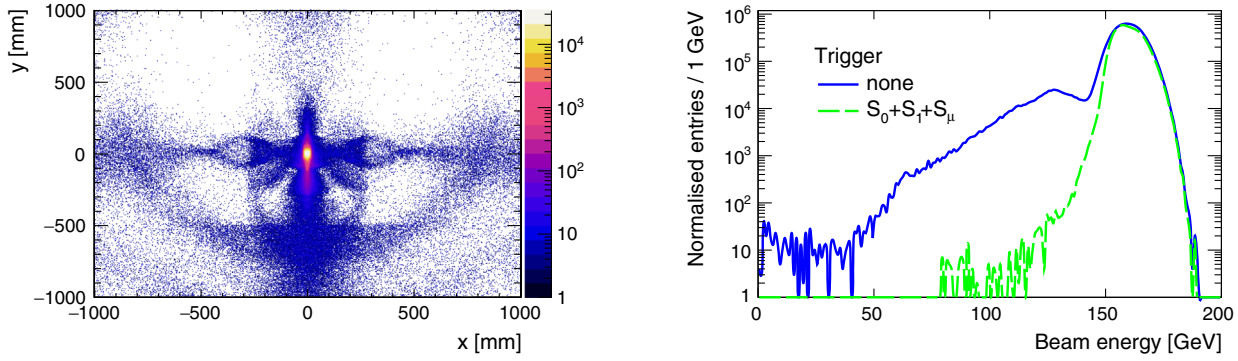

FIG. 3. Beam profiles at the entrance of the NA64μ setup as obtained through the TRANSPORT [50], TURTLE [51] and HALO [52] software [46] for (left) beam spatial distribution and (right) beam energy spectrum with no trigger (blue) and (green) trigger $S_0 + S_1 + S_\mu$.

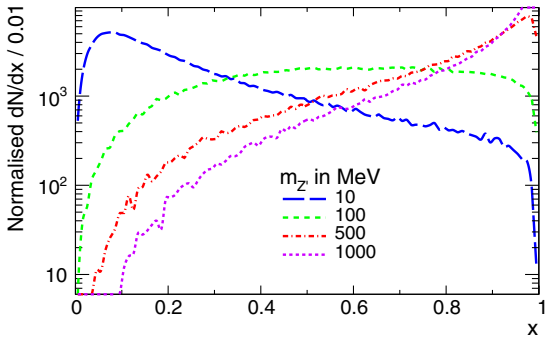

FIG. 4. Normalized energy spectra of the Z' vector boson for different masses obtained from GEANT4 [48] using the DMG4 [49] package. The mixing strength is $\epsilon = g'/\sqrt{4\pi\alpha} = 10^{-4}$, where $\alpha = 1/137$. See Ref. [40] for more details.

the Z' vector boson is simulated using the fully GEANT4-compatible DMG4 package [49]. Dark matter observables, such as the total cross-section production and the differential cross sections are correspondingly implemented according to the Weiszäcker-Williams (WW) phase-space approximation as discussed in Ref. [40]. The program selects an event where the Z' production should occur according to the total cross section, and then both its fractional energy, x, and emission angle, θ, are accurately sampled using a Von-Neumann accept-reject sampling algorithm. The typical energy spectra of a Z'-strahlung vector boson is shown in Fig. 4 for the mass range 10 MeV to 1 GeV.

C. Background

Missing energy/momentum experiments such as NA64μ rely not only on a robust detector hermeticity in order to avoid events with large missing energy appearing because some particles escaped detection due to acceptance, but also on a precise momentum reconstruction. Many processes, such as hard muon nuclear interactions in the ECAL, hadron admixture in the M2 beam line, or mismatch in momentum reconstruction, can affect the likelihood to truly observe a Z'-strahlung process. In the following paragraphs, the full study of those main background contributions is covered, being carried out through detailed MC simulations.

Muons usually behave as MIPs, thus most of them traverse the whole setup with nominal momentum $\sim$160 GeV/c, with small energy deposit in the calorimeters ($E_{\mathrm{ECAL}} \sim 0.5$ GeV, $E_{\mathrm{HCAL}} \sim 2.3$ GeV). On the opposite, scattered muons accompanied by Z' emission are identified with energy $E'_\mu \leq 0.5E_0 \simeq 80$ GeV. Accurate momentum reconstruction thus allows to discriminate between possible signal candidates and SM muon events. The muon momentum is reconstructed both upstream of the target and downstream of the ECAL through a series of magnetic spectrometers. To account for multiple scattering (material) effects as well as tracking detector resolution, the precision on momentum reconstruction is estimated using the Kalman-filter-based GENFIT toolkit [54] to be $\Delta p/p \sim 3\%$. The mismeasurement, and thus misidentification between Z'-strahlung and SM muons, is extracted from the exponential tails of the momentum residuals distribution. Through extrapolation, the probability of a 160 GeV SM muon to be reconstructed with momentum $\leq$80 GeV is $\lesssim 10^{-12}$ per muon on target (MOT). This result is obtained assuming that in particular selection criterium (ii) holds, i.e., a single hit per tracking detectors. In the case of more than one hit per tracker, the Micromegas detector inefficiency should be taken into account. An example of such physics processes is highly energetic secondaries produced by muons in the tracker material through ionization, $\mu e \to \mu e$, accompanied by a poorly detected parent muon, and thus yielding a reconstructed momentum with energy $<$100 GeV. The probability for such an event to happen is estimated from the full sample of simulated muons, taking into account the values for Micromegas trackers inefficiency ($\sim$0.02) extracted by previous NA64e run data, and assuming that in the second tracker downstream MS2 there is more than one hit. From the simulations, a conservative value of $\leq 10^{-11}$ per MOT is obtained, and can be further reduced by placing additional n trackers downstream, with a factor $\sim 0.02^n$.

In the case of NA64μ, the level of hermeticity of the detectors is inferred in the plane defined by the muon energy after ECAL and the total energy deposited in the calorimeter (ECAL, VHCAL and HCAL), $(E'_\mu; E_{\mathrm{CAL}})$, as shown in Fig. 5. Whereas region A corresponds to events with large energy deposit in the HCAL and the diagonal B to events with energy deposited in the ECAL, the bulk C is associated to events with energy deposition in the calorimeters compatible with a MIP. Thus a high level of hermeticity is reached for all events lying within those three regions. On the other side, poor detector hermeticity due to geometrical acceptance or dead material can lead to events with large missing energy, and thus leakage towards the signal box defined in the region D (red box) of Fig. 5 ($E_{\mathrm{CAL}} \leq 20$ GeV; $E'_\mu \leq 80$ GeV). From the distribution extrapolation in the plane $(E'_\mu; E_{\mathrm{CAL}})$, the probability of leakage in region D due to non-hermeticity (i.e., detector acceptance) is estimated to be $\lesssim 10^{-12}$ per MOT.

Apart from geometrical properties of the detectors, and thus acceptance, two main sources of physical background contribute to events with large missing energy. The first one arises from hadron admixture in the M2 beam line, typically charged and neutral hadrons, such as π^-, K^- and $K^0_{L(s)}$, and their subsequent (semi)leptonic decays along the setup. The level of contamination is measured with a set of beryllium absorbers in the beam line, and found to be $P_h = \pi/\mu \sim 10^{-6}$, with $K/\pi \sim 0.03$ [39]. To estimate the hadron decay probability, $P_{h\to X}$, and the

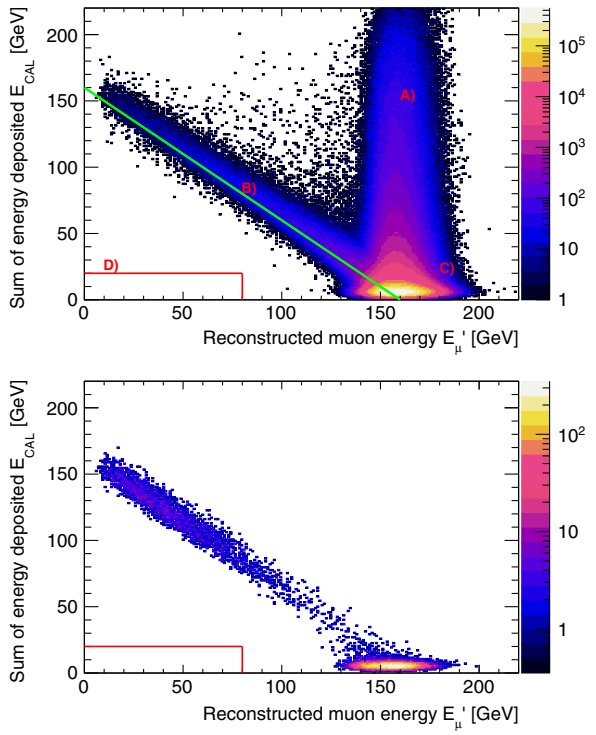

FIG. 5. Hermeticity plane defined by the reconstructed muon energy after the ECAL and the total energy deposit in the calorimeters, $(E'_\mu; E_{\mathrm{CAL}} = E_{\mathrm{ECAL}} + E_{\mathrm{VHCAL}} + E_{\mathrm{HCAL}})$, for SM muons with a single reconstructed track (one hit per Micromegas) assuming (top) trigger in counters S_0, S_1 and S_μ and (bottom) trigger in all counters, no energy deposit in the vetos, VHCAL and HCAL. The total number of simulated muons corresponds to $N_{\mathrm{MOT}} = 10^8$. Whereas region A, B and C correspond to regions compatible with SM-related energy deposit, region D defines the interesting parameter space compatible with Z'-strahlung events (see text).

related level of background, hadrons are simulated at the end of the COMPASS BMS to account for particle misidentification through momentum reconstruction. From MC simulations, along the typical distance to the active target of ∼36 m, it is found that $P_{K^-\to X} \sim \mathcal{O}(10^{-3})$, whereas $P_{\pi^-,K^0_L\to X} \sim \mathcal{O}(10^{-4})$. Thus, the total number of decay hadrons before the entrance of the setup is estimated through $N_{h\to X} = N_{\mathrm{MOT}} \times P_h \times P_{h\to X}$, which is $\sim\mathcal{O}(10^{-10}$–$10^{-11})$ per MOT. From those in-flight decays, background is associated to events with final state muons in the decay products, namely $h \to \mu^- X$, where X is mostly associated to a neutrino in the case of π^- and K^-, susceptible to carry away a large fraction of its parent hadron energy, thus mimicking a Z'-strahlung event with missing energy. For such a distance, the probability of kaons decaying to muons through the purely leptonic channel, $K^- \to \mu^-\bar{\nu}_\mu$, is about $P_{K^-\to\mu^-} \simeq 0.018$. For final state muons with energy $E_\mu < 100$ GeV, this probability reduces to $P_{K^-\to\mu^-}(E_\mu < 100\ \mathrm{GeV}) \simeq 0.011$. In the case of pion decays, this probability is strongly reduced because of the kinematics of the process. The overall probability for such a process, given the kaon contamination of the beam, is estimated at the level of 3.3×10^{-10} per MOT. For the full set of selection criteria, this background reduces to 1.1×10^{-11} per MOT. Such background can be further reduced by the mean of additional absorbers in the M2 beam line. For a $3.8\lambda_I = 150$ cm aluminum absorber, this probability is reduced by a factor $e^{-3.7} \simeq 0.023$. Additionally, using a dedicated magnetic spectrometer just before the active target [28,37] reduces the effective hadron decay length to 4 m, thus suppressing further this background by at least an order of magnitude according to simulations.

The second important source of background contributing to missing energy events originates from leading hadron production in the target. Those arise from muon nuclear interactions, $\mu^- N \to \mu^- h X$, within the ECAL material, with the outgoing hadron carrying away a significant fraction of the primary muon energy ($E_h \geq 80$ GeV). Such events can then leak through [punch through (PT)] the detector elements downstream of the target, with two possible scenarios mimicking a signal event: (i) the low energy outgoing muon is poorly detected and the leading charged hadrons deposit an energy compatible with the one of a MIP ($E_{\mathrm{HCAL}} \sim 2.5$ GeV) in the HCAL module; (ii) the outgoing muon is reconstructed with low energy and the neutral hadron traverses the HCAL modules undetected ($E_{\mathrm{HCAL}} \sim 0.1$ GeV). The probability for leading hadron production in the target is estimated through MC simulations to be 10^{-6} per MOT. Similarly, the probability for punching through a single or multiple HCAL module(s) is estimated with simulations and compared to available experimental data [55–57]. In the case of a single module, the effect of punch-through charged/neutral high energy hadrons—mostly π, K and neutrons n—appears as a peak in the low-energy end of the HCAL energy deposited spectrum. By extrapolating the low-end region of the spectrum, the PT probability for a single module corresponds to $\lesssim 10^{-2}$ per incoming hadron. A similar analysis extended to two and four modules yields a probability of $\lesssim 10^{-6}$ and $\lesssim 10^{-11}$ respectively. The overall total probability of producing a leading hadron which subsequently punches through two HCAL modules is thus estimated to be $\lesssim 10^{-12}$ per MOT.

For completeness to this study, muon electromagnetic interactions within the target also constitute a possible source of background, especially if visible decays of Z' are inferred (typically $Z' \to \mu^+\mu^-$). The main process is dimuons production through the emission of a real photon (Bethe-Heitler mechanism), $\mu^- N \to \mu^- N\gamma$; $\gamma \to \mu^+\mu^-$. Other mechanisms responsible for such dilepton production, although more suppressed, are the production of dimuon through a virtual photon (Trident process) or through highly energetic knock-on electrons (see e.g., Ref. [58–61]). The dimuon yield, suppressed by a factor

TABLE I. Main sources of background and expected background level per muons on target (MOT).

Source of background	Level per MOT
Hadron in-flight decay	$\lesssim 10^{-11}$
Momentum mismatch	$\lesssim 10^{-12}$
Detector non-hermeticity	$\lesssim 10^{-12}$
Single-hadron punch through	$\lesssim 10^{-12}$
Dimuon production	$< 10^{-12}$
Total (conservatively)	$\lesssim 10^{-11}$

of $(m_e/m_\mu)^5$ compared to electron bremsstrahlung, is estimated through MC simulations to be $\sim 10^{-7}$ per MOT. Because of the phase space associated to this process, final state muons can be efficiently rejected through the double/triple MIP signature in the HCAL modules, as well as within the tracking detectors. For the typical set of cuts used within this framework, possible background due to dimuons production is rejected at the level of $<10^{-12}$ per MOT.

Combining all of the above main sources of background, the experiment is expected to be background free at the level of $\sim 10^{11}$ MOTs (see Table I).

IV. FUTURE SENSITIVITY TO THE $(g-2)_\mu$

The signal yield of invisible decay of Z' to SM neutrinos, $Z' \to \bar{\nu}\nu$, can be estimated according to [37,40] such that

$$N_{Z'}^{(\bar{\nu}\nu)} = N_{\mathrm{MOT}} \cdot \frac{\rho \mathcal{N}_A}{A} \cdot \sum_i \sigma_{\mathrm{tot}}(E_\mu^i) \Delta L_i \cdot \mathrm{Br}(Z' \to \bar{\nu}\nu), \quad (6)$$

where $\mathcal{N}_A$ is the Avogadro number, ρ is the target density and A the target atomic weight, ΔL_i is the ith step length of the muon with energy E_μ^i within the target, and σ_{tot} the total cross section for Z' emission. The 90% confidence level upper limit on g' is calculated using Eq. (6), thus requiring $N_{Z'}^{(\bar{\nu}\nu)} > 2.3$ events, in the $(m_{Z'}, g')$ parameter space. The corresponding results are shown in Fig. 6 for $N_{\mathrm{MOT}} = 10^{11}$ assuming the selection criteria (i)–(iv) and a single scattered muon with energy $E'_\mu \leq 80$ GeV. Also shown is the values of g' and $m_{Z'}$ necessary to explain the muon $(g-2)_\mu$ within the 2σ band. It can be seen that for $N_{\mathrm{MOT}} \geq 10^{11}$, the parameter space necessary to explain the muon anomalous magnetic moment is fully covered. Additionally, it is also shown that with 10^{11} MOT, NA64μ is also sensitive to the parameters space region explaining the XENON1T excess [62].

For completeness, existing experimental bounds on Z' from the gauge extension $L_\mu - L_\tau$ theory are shown for neutrino trident production, $\nu N \to \nu N \mu\mu$, with the CCFR experiment [63,64], as well as from neutrino-electron scattering with the BOREXINO experiment [65,66]. Also shown are experimental constraints from electron-positron colliders with the *BABAR* [67] and Belle-II [68] experiments. As a comparison, projected sensitivities for Dune [72,73], Belle-II [74] and M^3 [38] are plotted alongside our estimated limits.

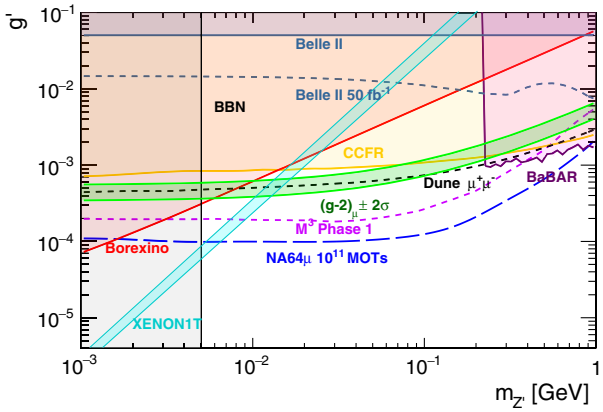

FIG. 6. Projected sensitivities for the invisible mode $Z' \to \bar{\nu}\nu$ in the $(m_{Z'}, g')$ parameter space for a total of 10^{11} MOT with the NA64μ experiment. The limits are given using the selection criteria (i)–(iv) and the requirement of the event lying in the signal box. The necessary $(m_{Z'}, g')$ values to explain the $(g-2)_\mu$ anomaly are shown within the 2σ green band, as well as the possible parameters to cover the XENON1T excess [62]. Also shown are current experimental constraints from CCFR [63,64], BOREXINO [65,66], *BABAR* [67] and Belle-II [68], together with the cosmological constraints from the big bang nucleosynthesis (BBN) [69–71]. Projected sensitivities from Dune [72,73], Belle-II [74] and M^3 [38] are also plotted.

V. CONCLUSION

In this work, we presented the expected sensitivity of the NA64μ experiment to a light Z' boson coupled to muons as a remaining low mass explanation of the $(g-2)_\mu$ muon anomaly. The minimal model based on the broken $U(1)_{L_\mu - L_\tau}$ symmetry is used as a benchmark in these studies. We focused on the optimization and design of the experimental setup for the first phase of the experiment dedicated to demonstrating the feasibility of the technique. The trigger efficiency and the detector hermeticity have been studied using a dedicated GEANT4-based MC simulation framework and a realistic M2 beam-optics simulation. A trigger using the scattered muon deflection after traversing the magnet spectrometer has been designed to keep the primary beam below 0.1% and a mass-dependent signal efficiency between 15%–35%. The low trigger efficiency for smaller masses is compensated by the mass dependence of the cross section. The main expected background sources arise from momentum misreconstruction in the two magnet spectrometers, hadron contamination and detector hermeticity. The results obtained from the simulation show that the background level is below 10^{-11} per MOT being dominated by the decay in flight of the remaining hadron contamination in the M2 beam line.

We also showed two methods which can potentially reduce this background by at least an order of magnitude. Finally, we studied the experiment projected sensitivities compared to present and future experiments aiming to perform similar searches. These first estimates based on simulations reveal that with 10^{11} MOT we can probe the region relevant to the $(g-2)_\mu$ anomaly, obtaining the most sensitive coverage for masses below 200 MeV. The presented simulation results and calculations are to be validated in the scheduled pilot run.

ACKNOWLEDGMENTS

We acknowledge the members of the NA64 collaboration for fruitful discussions, in particular, N. V. Krasnikov. The work of P. Crivelli, E. Depero, L. Molina Bueno and H. Sieber is supported by ETH Zürich and SNSF Grants No. 169133, No. 186181, No. 186158 and No. 197346 (Switzerland). The work of D. V. Kirpichnikov on MC simulation of Z' emission is supported by the Russian Science Foundation RSF Grant No. 21-12-00379.

[1] B. Abi *et al.* (Muon $g-2$ Collaboration), Measurement of the Positive Muon Anomalous Magnetic Moment to 0.46 ppm, Phys. Rev. Lett. **126**, 141801 (2021).
[2] T. Aoyama *et al.*, The anomalous magnetic moment of the muon in the Standard Model, Phys. Rep. **887**, 1 (2020).
[3] T. Aoyama, M. Hayakawa, T. Kinoshita, and M. Nio, Complete Tenth-Order QED Contribution to the Muon $g-2$, Phys. Rev. Lett. **109**, 111808 (2012).
[4] T. Aoyama, T. Kinoshita, and M. Nio, Theory of the anomalous magnetic moment of the electron, Atoms **7**, 28 (2019).
[5] A. Czarnecki, W. J. Marciano, and A. Vainshtein, Refinements in electroweak contributions to the muon anomalous magnetic moment, Phys. Rev. D **67**, 073006 (2003); **73**, 119901(E) (2006).
[6] C. Gnendiger, D. Stöckinger, and H. Stöckinger-Kim, The electroweak contributions to $(g-2)_\mu$ after the Higgs-boson mass measurement, Phys. Rev. D **88**, 053005 (2013).
[7] M. Davier, A. Hoecker, B. Malaescu, and Z. Zhang, Reevaluation of the hadronic vacuum polarization contributions to the Standard Model predictions of the muon $g-2$ and $\alpha(m_Z^2)$ using newest hadronic cross-section data, Eur. Phys. J. C **77**, 827 (2017).
[8] A. Keshavarzi, D. Nomura, and T. Teubner, Muon $g-2$ and $\alpha(M_Z^2)$: A new data-based analysis, Phys. Rev. D **97**, 114025 (2018).
[9] G. Colangelo, M. Hoferichter, and P. Stoffer, Two-pion contribution to hadronic vacuum polarization, J. High Energy Phys. 02 (2019) 006.
[10] M. Hoferichter, B.-L. Hoid, and B. Kubis, Three-pion contribution to hadronic vacuum polarization, J. High Energy Phys. 08 (2019) 137.
[11] M. Davier, A. Hoecker, B. Malaescu, and Z. Zhang, A new evaluation of the hadronic vacuum polarization contributions to the muon anomalous magnetic moment and to $\alpha(m_Z^2)$, Eur. Phys. J. C **80**, 241 (2020); **80**, 410(E) (2020).
[12] A. Keshavarzi, D. Nomura, and T. Teubner, $g-2$ of charged leptons, $\alpha(M_Z^2)$, and the hyperfine splitting of muonium, Phys. Rev. D **101**, 014029 (2020).
[13] A. Kurz, T. Liu, P. Marquard, and M. Steinhauser, Hadronic contribution to the muon anomalous magnetic moment to next-to-next- to-leading order, Phys. Lett. B **734**, 144 (2014).
[14] K. Melnikov and A. Vainshtein, Hadronic light-by-light scattering contribution to the muon anomalous magnetic moment reexamined, Phys. Rev. D **70**, 113006 (2004).
[15] P. Masjuan and P. Sánchez-Puertas, Pseudoscalar-pole contribution to the $(g_\mu-2)$: A rational approach, Phys. Rev. D **95**, 054026 (2017).
[16] G. Colangelo, M. Hoferichter, M. Procura, and P. Stoffer, Dispersion relation for hadronic light-by-light scattering: two-pion contributions, J. High Energy Phys. 04 (**2017**) 161.
[17] M. Hoferichter, B.-L. Hoid, B. Kubis, S. Leupold, and S. P. Schneider, Dispersion relation for hadronic light-by-light scattering: pion pole, J. High Energy Phys. 10 (2018) 141.
[18] A. Gérardin, H. B. Meyer, and A. Nyffeler, Lattice calculation of the pion transition form factor with $N_f=2+1$ Wilson quarks, Phys. Rev. D **100**, 034520 (2019).
[19] J. Bijnens, N. Hermansson-Truedsson, and A. Rodríguez-Sánchez, Short-distance constraints for the HLbL contribution to the muon anomalous magnetic moment, Phys. Lett. B **798**, 134994 (2019).
[20] G. Colangelo, F. Hagelstein, M. Hoferichter, L. Laub, and P. Stoffer, Longitudinal short-distance constraints for the hadronic light-by-light contribution to $(g-2)_\mu$ with large-N_c Regge models, J. High Energy Phys. 03 (2020) 101.
[21] T. Blum, N. Christ, M. Hayakawa, T. Izubuchi, L. Jin, C. Jung, and C. Lehner, Hadronic Light-by-Light Scattering Contribution to the Muon Anomalous Magnetic Moment from Lattice QCD, Phys. Rev. Lett. **124**, 132002 (2020).
[22] G. Colangelo, M. Hoferichter, A. Nyffeler, M. Passera, and P. Stoffer, Remarks on higher-order hadronic corrections to the muon $g-2$, Phys. Lett. B **735**, 90 (2014).
[23] M. Lindner, M. Platscher, and F. S. Queiroz, A call for new physics: The muon anomalous magnetic moment and lepton flavor violation, Phys. Rep. **731**, 1 (2018).
[24] D. Stöckinger, The muon magnetic moment and new physics, Hyperfine Interact. **214**, 13 (2013).
[25] J. P. Miller, R. Eduardo de, B. L. Roberts, and D. Stäckinger, Muon $(g-2)$: Experiment and Theory, Annu. Rev. Nucl. Part. Sci. **62**, 237 (2012).

[26] R. Capdevilla, D. Curtin, Y. Kahn, and G. Krnjaic, Systematically Testing Singlet Models for $(g-2)_\mu$, arXiv:2112.08377.

[27] S. N. Gninenko and N. V. Krasnikov, The muon anomalous magnetic moment and a new light gauge boson, Phys. Lett. B **513**, 119 (2001).

[28] S. N. Gninenko, N. V. Krasnikov, and V. A. Matveev, Muon $g-2$ and searches for a new leptophobic sub-GeV dark boson in a missing-energy experiment at CERN, Phys. Rev. D **91**, 095015 (2015).

[29] C.-Y. Chen, M. Pospelov, and Y.-M. Zhong, Muon beam experiments to probe the dark sector, Phys. Rev. D **95**, 115005 (2017).

[30] S. N. Gninenko and N. V. Krasnikov, Probing the muon $g_\mu-2$ anomaly, $L_\mu-L_\tau$ gauge boson and Dark Matter in dark photon experiments, Phys. Lett. B **783**, 24 (2018).

[31] D. V. Kirpichnikov, V. E. Lyubovitskij, and A. S. Zhevlakov, Implication of hidden sub-GeV bosons for the $(g-2)_\mu$, ^{8}Be-^{4}He anomaly, proton charge radius, EDM of fermions, and dark axion portal, Phys. Rev. D **102**, 095024 (2020).

[32] D. W. P. Amaral, D. G. Cerdeño, A. Cheek, and P. Foldenauer, Confirming $U(1)_{L_\mu-L_\tau}$ as a solution of $(g-2)_\mu$ with neutrinos, Eur. Phys. J. C **81**, 861 (2021).

[33] R. Foot, New physics from electric charge quantization?, Mod. Phys. Lett. A **06**, 527 (1991).

[34] X. G. He, G. C. Joshi, H. Lew, and R. R. Volkas, New-Z phenomenology, Phys. Rev. D **43**, R22 (1991).

[35] X.-G. He, G. C. Joshi, H. Lew, and R. R. Volkas, Simplest Z model, Phys. Rev. D **44**, 2118 (1991).

[36] S. Baek and P. Ko, Phenomenology of $U(1)_{L_\mu-L_\tau}$ charged dark matter at PAMELA/ FERMI and colliders, J. Cosmol. Astropart. Phys. 10 (2009) 011.

[37] D. Banerjee *et al.* (NA64 Collaboration), Proposal for an experiment to search for dark sector particles weakly coupled to muon at the SPS, Report No. CERN-SPSC:2019-002/ SPSC-P-359, 2019, https://cds.cern.ch/record/2653581?ln=en.

[38] Y. Kahn, G. Krnjaic, N. Tran, and A. Whitbeck, M^3: a new muon missing momentum experiment to probe $(g-2)_\mu$ and dark matter at Fermilab, J. High Energy Phys. 09 (2018) 153.

[39] N. Doble, L. Gatignon, G. von Holtey, and F. Novoskoltsev, The upgraded muon beam the SPS, Nucl. Instrum. Methods Phys. Res., Sect. A **343**, 351 (1994).

[40] D. V. Kirpichnikov, H. Sieber, L. Molina Bueno, P. Crivelli, and M. M. Kirsanov, Probing hidden sectors with a muon beam: Total and differential cross sections for vector boson production in muon bremsstrahlung, Phys. Rev. D **104**, 076012 (2021).

[41] S. Andreas, S. V. Donskov, P. Crivelli, A. Gardikiotis, S. N. Gninenko, N. A. Golubev, F. F. Guber, A. P. Ivashkin, M. M. Kirsanov, N. V. Krasnikov, V. A. Matveev, Y. V. Mikhailov, Y. V. Musienko, V. A. Polyakov, A. Ringwald, A. Rubbia, V. D. Samoylenko, Y. K. Semertzidis, and K. Zioutas, Proposal for an Experiment to Search for Light Dark Matter at the SPS, arXiv:1312.3309.

[42] S. N. Gninenko, Search for MeV dark photons in a light-shining-through-walls experiment at CERN, Phys. Rev. D **89**, 075008 (2014).

[43] S. N. Gninenko, D. V. Kirpichnikov, M. M. Kirsanov, and N. V. Krasnikov, Search for MeV dark photons in a light-shining-through-walls experiment at CERN, Phys. Lett. B **796**, 117 (2019).

[44] S. N. Gninenko, D. V. Kirpichnikov, and N. V. Krasnikov, Probing millicharged particles with NA64 experiment at CERN, Phys. Rev. D **100**, 035003 (2019).

[45] S. Gninenko, S. Kovalenko, S. Kuleshov, V. E. Lyubovitskij, and A. S. Zhevlakov, Deep inelastic $e-\tau$ and $\mu-\tau$ conversion in the NA64 experiment at the CERN SPS, Phys. Rev. D **98**, 015007 (2018).

[46] J. Bernhard *et al.*, Studies for new experiments at the CERN m2 beamline within physics beyond colliders: AMBER/ COMPASS++, NA64μ, MuonE, AIP Conf. Proc. **2249**, 030035 (2020).

[47] P. Abbon *et al.* (COMPASS Collaboration), The COMPASS experiment at CERN, Nucl. Instrum. Methods Phys. Res., Sect. A **577**, 455 (2007).

[48] S. Agostinelli *et al.* (GEANT4 Collaboration), GEANT4 a simulation toolkit, Nucl. Instrum. Methods Phys. Res., Sect. A **506**, 250 (2003).

[49] M. Bondi, A. Celentano, R. R. Dusaev, D. V. Kirpichnikov, M. M. Kirsanov, N. V. Krasnikov, L. Marsicano, and D. Shchukin, Fully Geant4 compatible package for the simulation of Dark Matter in fixed target experiments, Comput. Phys. Commun. **269**, 108129 (2021).

[50] K. L. Brown *et al.*, TRANSPORT: A computer program for designing charged-particle beam-transport systems (CERN, Geneva, 1980), https://cds.cern.ch/record/133647?ln=en.

[51] K. L. Brown and F. C. Iselin, DECAY TURTLE (Trace Unlimted Rays Through Lumped Elements): A computer program for simulating charged-particle beam transport systems, including decay calculations (CERN, Geneva, 1974), https://cds.cern.ch/record/186178?ln=en.

[52] C. Iselin, HALO: A computer program to calculate muon halo, Report No. CERN 74-17 Laboratory II, 1974, https://inis.iaea.org/search/search.aspx?orig_q=RN:6175777.

[53] M. Dobbs and J. B. Hansen, The HepMC C++ Monte Carlo Event Record for High Energy Physics, Report No. ATL-SOFT-2000-001, 2000, https://inspirehep.net/literature/553387.

[54] J. Rauch and T. Schlüter, GENFIT a Generic Tracking Fitting Toolkit, J. Phys. Conf. Ser. **608**, 012042 (2015).

[55] S. P. Denisov, S. V. Donskov, Y. P. Gorin, R. N. Krasnokutsky, A. I. Petrukhin, Y. D. Prokoshkin, and D. A. Stoyanova, Absorption cross sections for pions, kaons, protons and antiprotons on complex nuclei in the 6 to 60 GeV/c momentum range, Nucl. Phys. **B61**, 62 (1973).

[56] M. Aalste, M. Andlinger *et al.*, Measurement of hadron shower punchthrough in iron, Z. Phys. C **60**, 1 (1993).

[57] P. H. Sandler *et al.*, Hadron-shower penetration depth and muon production by hadrons of 40, 70, and 100 GeV, Phys. Rev. D **42**, 759 (1990).

[58] N. Chaudhuri and M. S. Sinha, Production of knock-on electrons by cosmic-ray muons underground (148 m w.e.), Nuovo Cimento (1955–1965) **35**, 13 (1965).

[59] S. Kelner *et al.*, About cross section for high-energy muon bremsstrahlung, MEphI Report No. MEPhI 024-95, 1995, https://inspirehep.net/literature/400124.

[60] A. Akhiezer and V. Berestestsky, *Quantum Electrodynamics* (Interscience Publishers, Geneva, 1965).
[61] A. G. Bogdanov, H. Burkhardt, V. N. Ivanchenko, S. R. Kelner, R. P. Kokoulin, M. Maire, A. M. Rybin, and L. Urban, Geant4 simulation of production and interaction of muons, IEEE Trans. Nucl. Sci. **53**, 513 (2006).
[62] D. Borah, M. Dutta, S. Mahapatra, and N. Sahu, Muon $(g-2)$ and XENON1T excess with boosted dark matter in $L_\mu - L_\tau$ model, Phys. Lett. B **820**, 136577 (2021).
[63] S. R. Mishra *et al.* (CCFR Collaboration), Neutrino tridents and $W-Z$ interference, Phys. Rev. Lett. **66**, 3117 (1991).
[64] W. Altmannshofer, S. Gori, M. Pospelov, and I. Yavin, Neutrino Trident Production: A Powerful Probe of New Physics with Neutrino Beams, Phys. Rev. Lett. **113**, 091801 (2014).
[65] Y. Kaneta and T. Shimomura, On the possibility of a search for the $L_\mu - L_\tau$ gauge boson at Belle-II and neutrino beam experiments, Prog. Theor. Exp. Phys. **2017**, 053B04 (2017).
[66] S. Gninenko and D. Gorbunov, Refining constraints from Borexino measurements on a light Z-boson coupled to $L_\mu - L_\tau$ current, Phys. Lett. B **823**, 136739 (2021).
[67] J. P. Lees *et al.* (*BABAR* Collaboration), Search for a muonic dark force at BABAR, Phys. Rev. D **94**, 011102 (2016).
[68] I. Adachi *et al.* (Belle-II), Search for an Invisibly Decaying Z Boson at Belle II in $e^+e^- \to \mu^+\mu^-(e^\pm\mu^\mp)$ Plus Missing Energy Final States, Phys. Rev. Lett. **124**, 141801 (2020).
[69] A. Kamada and H.-B. Yu, Coherent propagation of PeV neutrinos and the dip in the neutrino spectrum at IceCube, Phys. Rev. D **92**, 113004 (2015).
[70] B. Ahlgren, T. Ohlsson, and S. Zhou, Comment on Is Dark Matter with Long-Range Interactions a Solution to All Small-Scale Problems at Λ Cold Dark Matter Cosmology?, Phys. Rev. Lett. **111**, 199001 (2013).
[71] M. Escudero, D. Hooper, G. Krnjaic, and M. Pierre, Cosmology with a very light $L_\mu - L_\tau$ gauge boson, J. High Energy Phys. 03 (2019) 071.
[72] P. Ballett, M. Hostert, S. Pascoli, Y. F. Perez-Gonzalez, Z. Tabrizi, and R. Z. Funchal, Zs in neutrino scattering at DUNE, Phys. Rev. D **100**, 055012 (2019).
[73] W. Altmannshofer, S. Gori, J. Martín-Albo, A. Sousa, and M. Wallbank, Neutrino tridents at DUNE, Phys. Rev. D **100**, 115029 (2019).
[74] M. Campajola (Belle-II Collaboration), Dark Sector first results at Belle II, Phys. Scr. **96**, 084005 (2021).